Characterization of the Rice Canopy Infested with Brown Spot Disease Using Field Hyperspectral Data

□ ZHAO Jinling[1,2], ZHANG Dongyan[1],
LUO Juhua[1], DONG Yingying[1],
YANG Hao[1], HUANG Wenjiang[1]†

1. Beijing Research Center for Information Technology in Agriculture, Beijing Academy of Agriculture and Forestry Sciences, Beijing 100097, China;

2. Institute of Remote Sensing Applications, Chinese Academy of Sciences, Beijing 100101, China

Abstract: Based on the field hyperspectral data from the analytical spectral devices (ASD) spectrometer, we characterized the spectral properties of rice canopies infested with brown spot disease and selected spectral regions and bands sensitive to four severity degrees (severe, moderate, light, and healthy). The results show that the curves' variation on the original and the first- and second-order derivative curves are greatly different, but the spectral difference in the near-infrared region is the most obvious for each level. Specifically, the peaks are located at 822, 738, and 793 nm, while the valleys are located at 402, 570, and 753 nm, respectively. The sensitive regions are between 430-520, 530-550, and 650-710 nm, and the bands are 498, 539, and 673 nm in the sensitivity analysis, while they are in the ranges of 401-530, 550-730 as well as at 498 nm and 678 nm in the continuum removal.

Key words: rice brown spot disease; sensitive bands; disease severity degree; derivative transformation spectra; continuum removal method; sensitivity analysis method

CLC number: S 127

0 Introduction

With the increasing influence of fluctuant climate changes, it has shown a continuing upward trend of natural disasters that have exerted a negative effect on agricultural production and grain safety. As one of the leading factors threatening sustainable development of agriculture, pathogen of disease can cause severe damage to grain crops, which often leads to crop yield loss and poor quality[1,2]. Paddy rice is one of the most important grain crops in the world as the staple food of mankind. However, different kinds of diseases and pests have greatly threatened the rice production. As one of the rice diseases, the brown spot has caused qualitative and quantitative damages on rice[3]. In order to effectively control rice diseases and reduce production loss, a large amount of fungicide was used; meanwhile, a series of environmental problems were induced such as soil, water, and air pollutions[4]. Therefore, it will be of great importance to site-specifically and quantitatively monitor the rice brown spot disease, which could enhance the ability of farmers to implement beneficial disease treatments and reduce the incidence of disease and the amount of chemical applications.

Rice brown spot (*Cochliobolus miyabeanus*) is an aggressive plant disease caused by Bipolaris oryzae Shoem (*Helminthosporium oryzae*), which is one of the seed-borne diseases of rice, found in the all stages of its growth from nursery to farm and causes qualitative and quantitative damages on rice[5]. This disease occurs in rice production areas all over the world and is one of the

most common diseases in China[6]. However, owing to high variability in space and time with respect to its occurrence, it is difficult to monitor the incidence and prevalence of rice diseases by field investigation and sampling analysis. Traditional disease survey is labor-intensive to collect sample plots and identify the types and infected severity by experienced agronomists. For small regions, this method can play a role to a certain degree, but it will be time-consuming and labor-intensive at large scale[7]. Conversely, remote sensing has the potential use as an effective and inexpensive technique to identify diseased plants at a field scale, mainly because infected plants have different spectral response compared with healthy plants, which provides the possibility of remote sensing technology to identify the diseased plants through quantitative analysis of their spectral differences[8,9].

When rice is infected with pathogens, its growth will be affected and the changes of external morphology will appear in the canopy due to internal damage in chlorophyll pigments and tissue structure, which furthermore affects the photosynthesis and metabolism. Consequently, the diseased rice will have different spectral features from healthy plants. Kobayashi *et al*[10] evaluated the rice panicle blast using ratios of rice reflectance from airborne multispectral radiometer. Feng *et al*[11] identified and classified the rice leaf blast using the multispectral imaging sensor including green, red, and near-infrared (NIR) bands. Qin and Zhang[12] examined the applicability of broadband high spatial resolution ADAR (airborne data acquisition and registration) remote sensing data to detect rice sheath blight, and it was clear that identification accuracy increases when infection reaches medium to severe levels. Summarizing the above studies, it can be found out that most of corresponding studies of rice diseases are to estimate the area and spatial distribution of their incidence based on the aerial multispectral images. Nevertheless, the identification accuracy and fine classification of rice diseases are greatly affected due to the lower spectral resolution for multispectral images. Therefore, it is extremely important to effectively and accurately monitor the infection levels of rice brown spot, which can be very helpful to correctly and timely spray fungicide in precision agricultural management. Additionally, the ground-based researches of rice disease can lay a theoretical foundation and provide validation data for diagnosing disease on large-scale farming system using aerial photography and satellite image. In this paper, based on the ground-based hyperspectral data acquired with an ASD (analytical spectral devices), the spectral characteristics of rice canopies infested with brown spot disease were explored and the regions and bands sensitive to such a disease were also identified.

1   Materials and Methods

The experiment was performed in the villages of Yuanjiang City, which is in the north of Hunan Province and located at 28°42′26″-29°11′17″N, 112°14′37″-112°56′20″E, with an altitude of around 80 m above sea level. An average annual rainfall is around 1,400 mm. The average total annual sunshine is 1,743.5 h and the frost free period lasts for 276 days. The mean annual temperature is 16.9 °C and the mean temperatures in January and July are 4.3 °C and 29.1 °C, respectively (*http://www. hnzptong.cn/xinwen/renwen/renwenzixun/2010-08-28-/833. html*). Due to its subtropical humid monsoon climate, it is very suitable for platting paddy rice.

1.1   Field Positioning and Used Equipment

A field survey was carried out during September 13-16, 2010. At this moment, it was just the heading stage of dual-season later rice when it was the key period to form yield. Firstly, 25 sample plots were predefined on the high-resolution image of Google Earth, and their coordinates were also recorded and inputted into a handheld global positioning system (GPS, Trimble® GeoXH) receiver with less than 1 m positioning accuracy. Subsequently, in situ investigation was made by taking a car with a GPS antenna integrated with Arcmap GPS navigation module. According to the real-time navigation trail, the target places can be found. When rice brown spot was found in the field, disease severity was classified under the help of experienced agriculturist. At the same time, the canopy spectra and relative chlorophyll content (SPAD values, arbitrary unit) were measured using the ASD FieldSpec FR2500 and the chlorophyll meter (Konica Minolta SPAD-502, Japan). With a field of view (FOV) of 25°, the device operates in the 350-2 500 nm spectral region with a spectral resolution of 3 nm at 700 nm and of 10 nm at 1 400 and 2 100 nm and at a sampling interval of 1.4 nm between 350-1 050 nm and of 2 nm in the range of 1 000-2 500 nm. SPAD-502 chlorophyll meter acquires the relative chlorophyll content by measuring leaf transmittance at 650 and 940 nm.

1.2   Acquisition of the Disease Severity Index (DSI)

Disease severity was assessed by the phytopathologists in the paddy field. It was estimated in accordance with the percentage of infested leaves per plot at the canopy level. For each plot, an area of 1×1 m was selected to

investigate the disease severity. Then, the number of leaves and disease spots were recorded and the DSI of rice brown spot was discerned according to Eq. (1):

$$DSI = \frac{\sum\limits_{i=1}^{n} S_i}{\sum\limits_{j=1}^{m} S_j} \qquad (1)$$

where S_i is the area of disease spot, S_j is the area of rice leaves, i is the diseased spot number per unit area, and j is the number of leaves per unit area.

As a result, 32 field survey points were collected, and Table 1 shows the DSI values for those sampling plots. By statistical analysis, DSI_{mean}, DSI_{max}, DSI_{min}, and $S.D._{DSI}$ (standard deviation for those DSI values) are 27, 70, 10 and 19.5, respectively. To classify the DSI levels, the mean was used as the basis and those with greater DSI than the mean were only averaged considering that there is not much difference among those DSI values less than the mean. The result shows that the mean is 16% and $S.D._{DSI}$ is 6.5 less than the mean, and they are 44% and 12.6 for those DSI values greater than the mean. Finally, based on the means, four severity levels were classified: D0 (5 plots, DSI=0%), healthy rice canopy; D1 (12 plots, DSI is between 0% and 27%), light level; D2 (8 plots, DSI is between 27% and 44%), moderate level; and D3 (7 plots, DSI is between 27% and 44%), severe level.

Table 1   The DSI values of 32 field survey points   %

Sampling no.	DSI	Sampling no.	DSI
1	23	17	0
2	31	18	34
3	0	19	18
4	52	20	28
5	15	21	57
6	0	22	0
7	70	23	42
8	46	24	21
9	8	25	17
10	20	26	47
11	0	27	23
12	38	28	29
13	16	29	10
14	39	30	17
15	55	31	15
16	61	32	36

1.3 Spectral Data Acquisition and Reflectance Conversion

The canopy-reflected spectra of healthy and infested rice were collected in the paddy fields under cloudless conditions between 11:00 and 14:30 Beijing local time using ASD spectrometer at 1 m above the canopy. Canopy spectra were measured at different disease severity levels for a total of 32 plots in the paddy fields. For each sample spot, two scans were made and a total of 10 replicate measurements were taken for each scan. Before and after measuring the rice canopy, a barium sulfate ($BaSO_4$) calibration panel was measured twice simultaneously with the target at the same position. As a result, 20 spectral samples were obtained from one plot and the average value of the two scans was used as the final reflectance. To enhance the comparison and reduce random errors, the reflectance values were averaged of all sampling plots for each level and four spectral curves were finally obtained.

When the original data were measured, further processing must be required to covert the radiance values to reflectance using reference panel. For the ASD reflectance conversion, ASD-viewspec Pro Version 6.0 was used to export original radiance values to Excel, and Eq. (2) was used to derive the converted reflectance using the ASD spectrometer:

$$R_t = \frac{Rad_t}{Rad_r} \times R_r \times 100\% \qquad (2)$$

where R_t is the target's calibrated reflectance using reference panel, Rad_t is the target's radiance values acquired by ASD spectrometer, Rad_r is the measured radiance values of reference panel, and R_r is the known reflectance of the reference panel.

1.4 Spectral Data Preprocessing and Spectral Transformation

Figure 1 is the technical flowchart of data preprocessing. Before the data are further analyzed, there are two things that have to be done. One is to exclude the abnormal values and the absorption bands of water vapor and the other is to smooth the spectral curves. To suppress instrumental and environmental noise in the converted data, reflectance data of rice canopies were firstly smoothed using a five-point moving average algorithm[13]. After the data preprocessing, derivative spectral analysis (DSA) was then performed with its little influence of soil background. Finally, two methods of sensitivity analysis[1] and the continuum removal[14] were utilized to select the sensitive bands and spectral regions concerning different disease levels. In this study, data analysis and drawing illustrations were carried out using the OriginPro 8 software.

Hyperspectral data from the ASD consist of hundreds of contiguous spectral bands, and they provide an opportunity to pursue sophisticated analysis and applications that are difficult to achieve using traditional multispectral data. However, the large data volume is
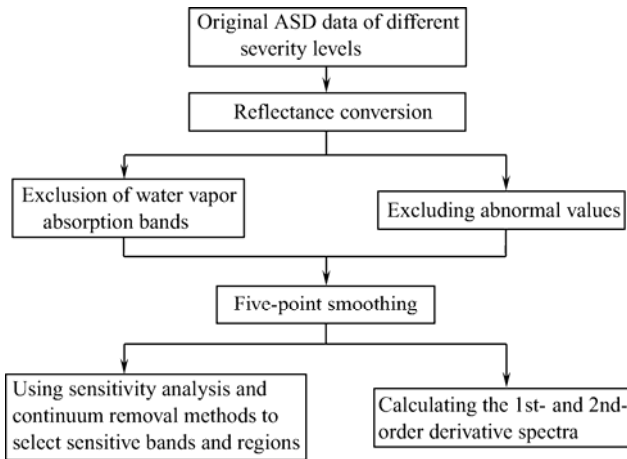
Fig. 1   Flowchart for data preprocessing

already a difficult issue to deal with. DSA algorithms can facilitate the extraction of "useful" information from hyperspectral data. It can reveal the essence by partially reducing the effect of atmosphere and the environmental background of vegetation (shadow, soil, etc.). Demetriades-Shah *et al* [15] introduced the detailed information about computation of the derivative spectra. Here, the first- and second-order derivative spectra were used to separate the severity levels of diseased rice canopies. The first-order derivative (the slope) provides information on the rate of change in reflectance with respect to wavelength, while the second-order derivative reveals the change in slope with respect to wavelength[1]. Eqs. (3) and (4) are the calculation formulae of the first- and second-order derivatives, respectively.

$$\rho'(\lambda_i) = \left[\rho(\lambda_{i+1}) - \rho(\lambda_{i-1})\right] \Big/ 2\Delta\lambda \qquad (3)$$

$$\rho''(\lambda_i) = \left[\rho'(\lambda_{i+1}) - \rho'(\lambda_{i-1})\right] \Big/ 2\Delta\lambda \qquad (4)$$

where λ_i is the wavelength at a certain band, $\rho(\lambda_i)$ is the reflectance at the wavelength of i, $\rho'(\lambda_i)$ is the first-order derivative at the wavelength of i, $\rho''(\lambda_i)$ is the second-order derivative at the wavelength of i, and $\Delta\lambda$ is the wavelength interval between neighboring bands.

Sensitivity analysis is to select sensitive bands, which is computed by diving the appropriate reflectance difference by the mean reflectance of uninfected rice to identify the wavelength at which reflectance is the most strongly affected by fungal infection (Eq. (5))[1]:

$$SS = (\rho_s - \rho_h)/\rho_h \qquad (5)$$

where SS is the spectral sensitivity, ρ_s is the reflectance of disease-stressed rice, and ρ_h is the reflectance of healthy rice canopy.

Carter showed that the reflectance difference was computed by subtracting the mean reflectance of the uninfected rice at each spectroradiometer channel to represent more clearly the reflectance response to the change of

disease occurrence[16].

Continuum is a polyline formed by connecting those peak points using a line on the original spectral curve, which requires exterior angle greater than 180º of the polyline on those peak points. Continuum removal is in essence an extrapolation of the baseline of the general curve, which fits a smoothed curve to the general trend to extend across the base of absorption bands. To allow comparison of individual absorption features from a common baseline, this method can normalize reflectance spectra[14]. The continuum is a convex hull fit over the top of a spectrum using straight line segments that connect local spectra maxima. Furthermore, the calculation equation of depth for an absorption band (D) is shown in Eq. (6):

$$D = 1 - R_b / R_c \qquad (6)$$

where R_b/R_c is the relative reflectance after continuum removal, R_b is the reflectance at the bottom (trough center point) of a band, and R_c is the continuum base and it is the value of this trough center point on the continuum.

The first and last spectral data are on the hull, so the first and last bands in the output continuum-removed data file are converted to 1.0. Kokaly and Clark[14] were the first researchers to use the method in vegetation studies when estimating nitrogen, lignin, and cellulose concentrations in dried ground leaves.

2   Results and Discussion

2.1   Spectral Reflectance Characteristics of Healthy and Infested Rice Canopy

Before analyzing the spectral characteristics of rice canopies infested with brown spot disease, the SPAD values were firstly used to diagnose the chlorophyll changes caused by such a disease. It is obvious that chlorophyll content decreases with the increase of infestation severity (Fig. 2). For the brown spot disease, the fungus causes brown, circular to oval spots on the coleoptile leaves of the seedlings. The spots on the leaf sheath and hulls are similar than those on the leaves. Additionally, the pathogen also attacks the coleoptiles, branches of the panicle, glumes, and grains, so the chlorophyll content will accordingly decrease.

Furthermore, the spectral reflectance curves were drawn on the basis of analyzing the chlorophyll changes. It is obvious that spectral curves are greatly affected in the spectral range of 1 350-1 450 nm, 1 780-2 000 nm and 2 350-2 500 nm due to the absorption of water vapor (Fig. 3(A)). Due to the existence of water vapor absorption,

some abnormal values were induced on the curves; unfortunately, the effective spectral curves were flattened. In order to reflect the real spectral characteristics, those bands must be excluded (Fig.3(B)). As shown in Fig.3(A), in the visible (VIS, 400-680 nm) and shortwave-infrared (SWIR, 1 500-1 750 nm) spectral ranges, it is difficult to differentiate the severity levels because of subtle magnitude changes. However, they are obvious in the NIR 760‐1 300 nm) region. The maximum and minimum values are at 402 and 822 nm, respectively, on the original spectra. Comparing healthy ones with diseased rice canopy, it can be found out that their spectra are obviously different and can be separated. The two illustrations of Figs. 2 and 3 provide a theoretical basis for identifying the disease severity degree of rice brown spot disease using remote sensing technique.
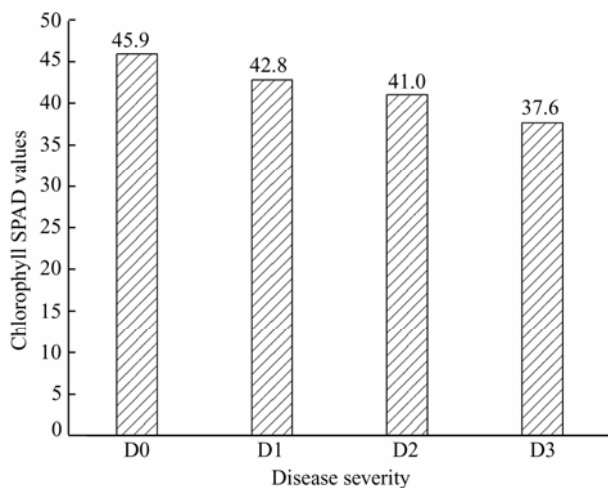

Fig. 2   **Comparison of the SPAD chlorophyll**
of four disease severity levels

After obtaining the preprocessed spectral curves, the first- and second-order derivative spectra were calculated to compare the difference among the sensitivity at their four severity levels. In order to improve the spectral characteristics, the adjacent-averaging method with six points of window was used to smooth the first-order derivative spectral curves (Fig. 4(A)). Comparatively, the second-order derivative is inherently noisier than the first-order derivative, so the adjacent-averaging method with 20 points of window was used (Fig. 4(B)). On the first-order derivative spectral curves, there are two reflectance peaks in the VIS and NIR spectral regions and they are at 523 and 738 nm for the healthy rice, respectively, while they are at 523 and 727 nm for the badly diseased rice, respectively. This phenomenon shows that the red edge appears in the wavelength of 680-750 nm, and the
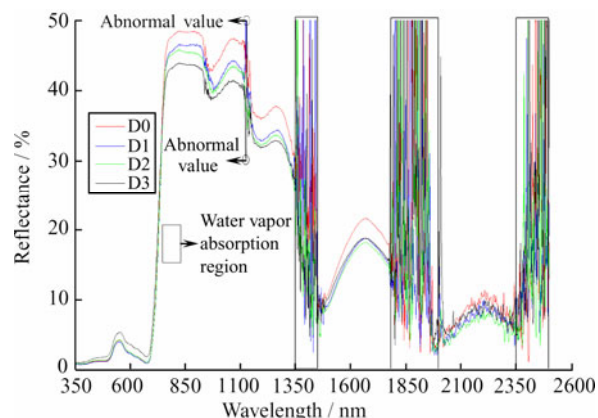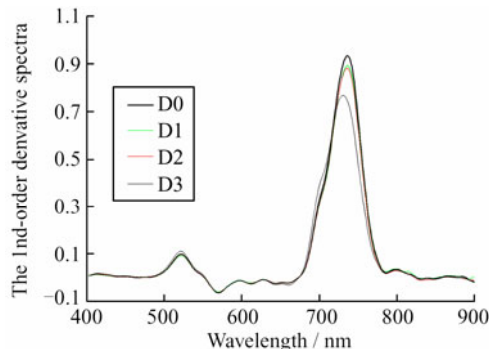

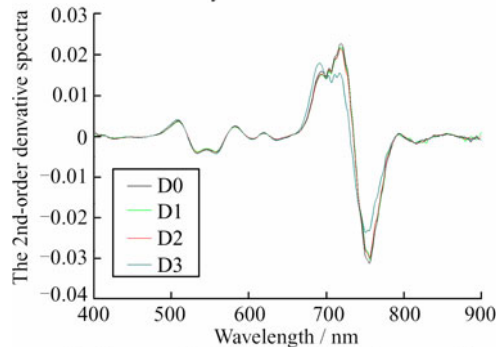(A) Original spectral curves of four severity levels
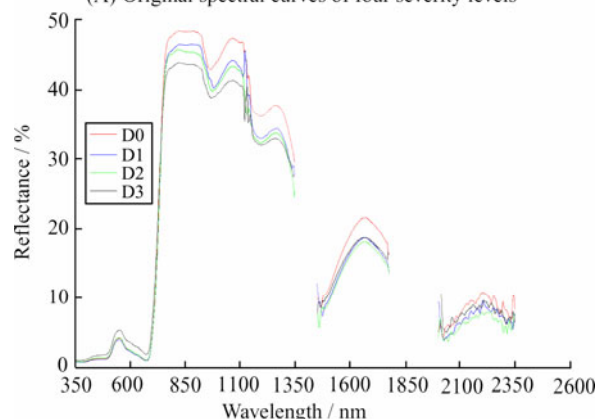
(B) Smoothed spectral curves of four severity levels after removing water vapor absorption bands

Fig. 3   **Comparison between original and preprocessed spectral curves of four severity disease levels**

(A) The smoothed 1st-order derivative spectral curves of four severity levels

(B) The smoothed 2nd-order derivative spectral curves of four severity levels

Fig. 4   **First- and second-order derivative spectra of four severity disease levels**

smallest reflectance spectrum is at 570 nm and the value is -0.072. For the second-order derivative spectra, the magnitude change is much bigger and there are more peaks and valleys than that of the first-order derivative spectra especially in the spectral range of 500-800 nm. At wavelength of 500-650 nm, the maximum and minimum magnitudes exist and they are located at 511 and 532 nm, respectively. While at wavelength of 650-800 nm, there are three reflectance peaks and two valleys. Their peaks are at approximately 692, 719, and 793 nm, respectively, while the valleys are at approximately 703 and 753 nm.

Summarizing the above analysis, it shows that the difference of spectral reflectance is significant for different disease severity levels, but they are obviously different in different spectral regions (VIS, NIR, and SWIR). Comparatively, the spectral difference in the NIR region is the most obvious. Especially, derivative spectra including the first- and second-order can more correctly illustrate the spectral characteristics between healthy and infested rice canopies with their insensitive features to the typical soil reflectance and atmospheric effects. The analysis results show that the absolute value of the derivative spectra generally decreased with the increase of severity degree, which is nearly consistent with the analysis of Liu *et al*.[1].

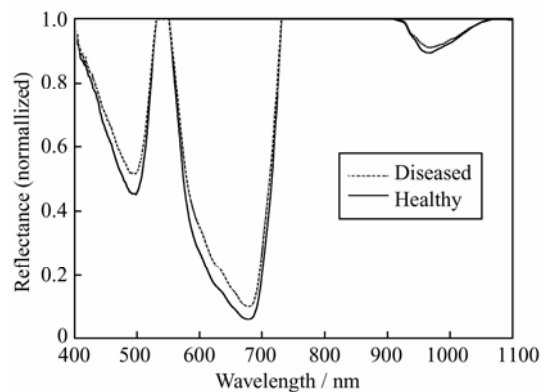## 2.2 Selection of Sensitive Bands and Spectral Regions

For the hyperspectral remote sensing data, sensitive bands are crucial to reduce data redundancy, select effective bands, and build a conversion model. Therefore, it is important to accurately pick up the most sensitive bands or spectral regions. In this study, sensitivity analysis and continuum removal methods were simultaneously used to select the sensitive bands and regions. It is obvious that the change magnitude decreases rapidly with the increasing infestation levels (Fig. 5(A)). Taking the D3 as an example, in the VIS and NIR regions (400-740 nm), the value of sensitivity is positive, which shows that the reflectance of disease-stressed rice is greater than that of healthy rice. Due to the influence of rice brown spot, near the blue bands (centered at 498 nm) and the red bands (centered at 673 nm), the increase of reluctance is more, while its increase is less near the green bands (centered at 539 nm). When the wavelength is greater than 673 nm, the value of sensitivity is positive, which shows that the reflectance of healthy rice is greater than that of diseased rice. In Fig. 5(A), the maximum value is 0.82 and located at 673 nm and the minimum value is -0.13 and located at 1 097 nm. According to the extreme peaks and valleys in the distribution of sensitivity curves,

the positions of sensitive bands and spectral regions can be specified where the spectral difference is great.

The continuum removal method can normalize reflectance spectra to the range between 0 and 1, so it allows the comparison of individual absorption features from a common baseline. As can be seen in Fig. 5(B), there are three regions: 400-530, 550-730, and 900-1 100 nm. However, the values of blue bands centered at 498 nm are less than that of from red to NIR bands centered at 678 nm. Comparatively, the bands centered at 976 nm have to be abandoned because of less payload information. In three absorption regions, the regional variation of 550-730 nm spectral range is largest than that of the two other regions, which indicates that this region will have a better effect in differentiating the severity degree of rice brown spot disease. Table 2 lists the selection results of sensitive spectral regions and bands, and it is obvious that they are extremely similar, except that it has one more region and band of sensitivity analysis than continuum removal. The phenomenon shows that there is no special close relationship between the selection of sensitive bands and regions and the algorithms.
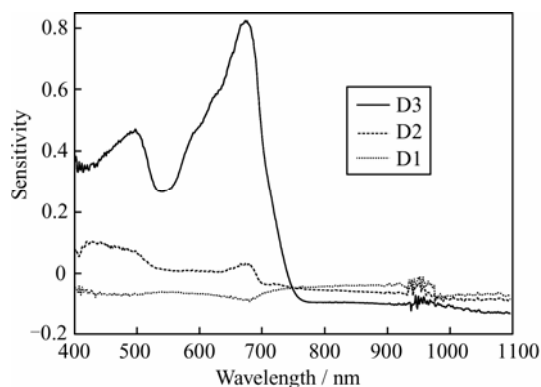
(A) Represents the identified spectral sensitive regions and bands using the sensitivity analysis method

(B) Represents the identified spectral sensitive regions and bands using the continuum removal method

Fig. 5 Selection of sensitive bands and spectral regions using the spectral transformation and continuum removal methods

Table 2   Selected sensitive spectral regions and bands using sensitivity analysis and continuum removal methods   nm

Analysis method	Sensitive spectral regions	Sensitive spectral bands
Sensitivity analysis	430-520, 530-550, 650-710	498, 539, 673
Continuum removal	401-530, 550-730	498, 678

3   Conclusion

This study aimed at characterizing the spectral reflectance of rice canopy infested with brown spot disease. Based on our analysis, we drew several conclusions as follows:

① Hyperspectral remote sensing technology can be used as an effective and inexpensive method to identify diseased plants at a field scale. When the original reflectance data were further analyzed, the abnormal values and water absorption bands must be firstly excluded due to the existence of instrumental and environmental noise.

② To clearly represent the spectral characteristics, the original reflectance and spectral transformation must be smoothed. Spectral derivative analysis can sharpen the spectral features, but the derivative orders must be correctly chosen.

③ The comparative study of two sensitive-bands selection methods show that the selected spectral regions and bands are similar, which shows that there is no special close relationship between method selection and identification results.

References

[1]   Liu Zhanyu, Huang Jingfeng, Tao Rongxiang. Characterizing and estimating fungal disease severity of rice brown spot with hyperspectral reflectance data [J]. *Rice Science*, 2008, **15**(3): 232-242.

[2]   Elibuyuk I O, Bostan H. Detection of a virus disease on Agaricus bisporus (white button mushroom) in Ankara, Turkey [J]. *International Journal of Agriculture and Biology*, 2010, **12**(4): 597-600.

[3]   Motlagh M R, Kaviani B. Characterization of New Bipolaris spp., the causal agent of rice brown spot disease in the north of Iran [J]. *International Journal of Agriculture and Biology*, 2008, **10**(6): 638-642.

[4]   West J S, Bravo C, Oberit R, *et al*. The potential of optical canopy measurement for targeted control of filed crop diseases [J]. *Annual Review of Phytopathology*, 2003, **41**(1): 593-614.

[5]   Safari-Motlagh M R, Padasht F, Hedjaroude G H. Rice brown spot disease in Guilan Province and the study of the reaction of some cultivars to the disease [J]. *Journal of Science and Technology of Agriculture and Natural Resources*, 2005, **9**(2): 171-183.

[6]   Liu Zhanyu, Huang Jingfeng, Shi Jingjing, *et al*. Characterizing and estimating rice brown spot disease severity using stepwise regression, principal component regression and partial least-square regression [J]. *Journal of Zhejiang University Science B*, 2007, **8**(10): 738-744.

[7]   Lucas J A. *Plant Pathology And Plant Pathogens* [M]. 3rd ed. Oxford, UK: Blackwell Science, 1998.

[8]   Zhang Minghu, Liu Xue, O'Neill M. Spectral discrimination of phytophthora infestans infection on tomatoes based on principle component and cluster analyses [J]. *International Journal of Remote Sensing*, 2002, **23**(6): 1095-1107.

[9]   Zhang Minghua, Qin Zhihao, Liu Xue, *et al*. Detection of stress in tomatoes induced by late blight disease in California, USA, using hyperspectral remote sensing [J]. *International Journal of Applied Earth Observation and Geoinformation*, 2003, **4**(4): 295-310.

[10] Kobayashi T, Kanda E, Kitada K, *et al*. Detection of rice panicle blast with multispectral radiometer and the potential of using airborne multispectral scanners [J]. *Phytopathology*, 2001, **91**(3): 316-323.

[11] Feng Lei, Chai Rongyao, Sun Guangming, *et al*. Identification and classification of rice leaf blast based on multi-spectral imaging sensor [J]. *Spectroscopy and Spectral Analysis*, **29**(10): 2730-2733.

[12] Qin Zhihao, Zhang Minghua. Detection of rice sheath blight for in-season disease management using multispectral remote sensing [J]. *International Journal of Applied Earth Observation and Geoinformation*, 2005, **7**(2): 115-128.

[13] Kobayashi T, Kanada E, Naito S, *et al*. Ratio of rice reflectance for estimating leaf blast severity with a multisectral radiometer [J]. *Journal of General Plant Pathology*, 2003, **69**(1): 17-22.

[14] Kokaly R F, Clark R N. Spectroscopic determination of leaf biochemistry using band-depth analysis of absorption features and stepwise multiple linear regression [J]. *Remote Sensing of Environment*, 1999, **67**(3): 267-287.

[15] Demetriades-Shah T H, Steven M D, Clark J A. High resolution derivative spectra in remote sensing [J]. *Remote Sensing of Environment*, 1990, **33**(1): 55-64.

[16] Carter G A. Primary and secondary effects of water content on the spectral reflectance of leaves [J]. *American Journal of Botany*, 1991, **78**(7): 916-924.

□